

## Effect of *in vivo* culture conditions on the proliferation and differentiation of rat adipose-derived stromal cells

Chao Wang <sup>a,b,c</sup>, Tian Xie <sup>d</sup>, Xiaoming Li <sup>e</sup>, Xue Lu <sup>a,b,c</sup>, Changxue Xiao <sup>a,b,c</sup>, Ping Liu <sup>f</sup>, Feng Xu <sup>a,b,c,\*</sup>, Bo Zhang <sup>f,\*\*</sup>

<sup>a</sup> Department of Intensive Care Unit, Children's Hospital of Chongqing Medical University, Chongqing 400014, China

<sup>b</sup> National Clinical Research Center for Child Health and Disorders, Ministry of Education Key Laboratory of Child Development and Disorders, Children's Hospital of Chongqing Medical University, Chongqing 400016, China

<sup>c</sup> Chongqing Key Laboratory of Pediatric Metabolism and Inflammation Diseases, Chongqing 400016, China

<sup>d</sup> Department of Radiology, Daping Hospital, Army Medical University, Chongqing 400042, China

<sup>e</sup> Department of Military Traffic Injury Prevention, Daping Hospital, Army Medical University, Chongqing 400042, China

<sup>f</sup> State Key Lab of Trauma, Burns and Combined Injury, Institute of Surgery Research, Daping Hospital, Army Medical University, Chongqing 400042, China

### ARTICLE INFO

#### Keywords:

Adipose-derived stromal cells (ADSCs)

Proliferation

Differentiation

Multipotency

RNA sequencing

### ABSTRACT

Adipose-derived stromal cells (ADSCs) are promising stem cell sources for tissue engineering and cell-based therapy. However, long-term *in vitro* expansion of ADSCs impedes stemness maintenance, which is partly attributed to deprivation of their original microenvironment. Incompetent cells limit the therapeutic effects of ADSC-based clinical strategies. Therefore, reconstructing a more physiologically and physically relevant niche is an ideal strategy to address this issue and therefore facilitates the extensive application of ADSCs. Here, we transplanted separated ADSCs into local subcutaneous adipose tissues of nude mice as an *in vivo* cell culture model. We found that transplanted ADSCs maintained their primitive morphology and showed improved proliferation and delayed senescence compared to those of cells cultured in an incubator. Significantly increased expression of stemness-related markers and multilineage differentiation abilities were further observed in *in vivo* cultured ADSCs. Finally, sequencing revealed that genes whose expression differed between ADSCs obtained under *in vivo* and *in vitro* conditions were mainly located in the extracellular matrix and extracellular space and that these genes participate in regulating transcription and protein synthesis. Moreover, we found that an Egr1 signaling pathway might exert a crucial impact on controlling stemness properties. Our findings might collectively pave the way for ADSC-based applications.

### 1. Introduction

Adipose-derived stromal cells (ADSCs) are emerging attractive mesenchymal stem cells (MSCs) for tissue repair and regenerative medicine. Benefiting from their high self-renewal capacity, multilineage

differentiation potential, and secretion of abundant bioactive factors, ADSCs have gradually played promising roles in a wide range of intractable diseases, including graft-versus-host disease (GVHD), Crohn's disease (CD), myocardial infarction (MI), acute respiratory distress syndrome (ARDS) and bone/cartilage defects (Zhao et al., 2022;

**List of Abbreviations:** ADSCs, adipose-derived stromal cells; MSCs, mesenchymal stromal cells; Con-ADSCs, fourth passage ADSCs; Vitro-ADSCs, ADSCs cultured in traditional incubator; Vivo-ADSCs, ADSCs transplanted and grown in the adipose tissues of nude mice; 2D, two-dimensional; 3D, three-dimensional; GFP, green fluorescence protein; FBS, fetal bovine serum; ECM, extracellular matrix; MTT, methylthiazolyl tetrazolium; CFU, colony-forming unit; HRP, horseradish peroxidase; RIPA, radioimmunoprecipitation assay; BCA, bicinchoninic acid; PVDF, polyvinylidene fluoride; TBST, Tris-buffered saline with Triton X-100; PFA, paraformaldehyde; PBS, phosphate buffered saline; DAPI, 2,4-amidinophenyl-6-indolecarbamidine dihydrochloride; SD, standard deviation; ANOVA, one-way analysis of variance; siRNA, small interfering RNA; qRT-PCR, quantitative reverse transcription polymerase chain reaction; RNA-seq, RNA sequencing; RGSC, Rat Genome Sequencing Consortium; DEGs, differentially expressed genes; GO, Gene Ontology; KEGG, Kyoto Encyclopedia of Genes and Genomes; Egr1, early growth response 1; Socs3, suppressor of cytokine signaling 3.

\* Corresponding author at: Department of Intensive Care Unit, Children's Hospital of Chongqing Medical University, Chongqing 400014, China.

\*\* Corresponding author.

E-mail addresses: [fengxu@cqmu.edu.cn](mailto:fengxu@cqmu.edu.cn) (F. Xu), [zhangbo67184@163.com](mailto:zhangbo67184@163.com) (B. Zhang).

<https://doi.org/10.1016/j.mad.2024.111935>

Received 22 January 2024; Received in revised form 4 April 2024; Accepted 11 April 2024

Available online 12 April 2024

0047-6374/© 2024 Elsevier B.V. All rights reserved.

Zhou et al., 2021; Ichikado et al., 2023; Zhuang et al., 2021). ADSCs are characterized by easy accessibility, abundant quantity, minimal trauma, low-risk sampling techniques, and a lower population doubling time than bone marrow MSCs and umbilical cord MSCs. To date, ADSCs have been shown to have greater benefit-to-risk effect on wound repair and tissue regeneration (e.g., skin, bone, and cartilage applications), where they have been shown to modulate immune and metabolic responses, suppress oxidative stress, and promote angiogenesis and differentiation (Zhou et al., 2019; Bacakova et al., 2018; Mazini et al., 2019). Overall, these features of ADSCs suggest their superiority in clinical application.

The therapeutic advantages of ADSCs have been reported to predominantly rely on their high cell number and high quality (Zhao et al., 2022; Fazekas et al., 2022; Gong et al., 2022; Song et al., 2018). Thus, extensive *in vitro* expansion of ADSCs is prerequisite for achieving the sufficient cell numbers required for preclinical and clinical use (Bacakova et al., 2018). However, long-term culture with serial passaging results in decreased proliferative ability, accumulated senescence, and loss of multilineage differentiation, which seriously impedes their therapeutic effects (Shuai et al., 2016; He et al., 2024; Wang et al., 2021). Therefore, exploring the optimal culture conditions for ADSCs is highly important.

The cellular microenvironment is generally identified as a pivotal complex regulating the stemness properties of ADSCs (Scadden, 2006; Jiang et al., 2023). Culturing ADSCs under optimized conditions by mimicking the original microenvironment is considered a feasible way to maintain stemness. In practice, two-dimensional (2D) culture methods involving exposure to cytokines, physiological hypoxia, and three-dimensional (3D) culture are routinely adopted. These methods are largely used to circumvent issues surrounding altered cellular properties and the deteriorative therapeutic benefits of excessively manipulated ADSCs (Zhou et al., 2021; Scadden, 2006; Jiang et al., 2023; Costa et al., 2021; Hu and Li, 2018; Rangasami et al., 2021). However, the components surrounding stem cells, including the extracellular matrix, oxygen, topography, secreted factors and other cellular components, function synergistically and dynamically, rather than independently, to retain the properties of ADSCs *in vivo* (Scadden, 2006; Jiang et al., 2023). Despite simulating one or several physical and chemical components, *in vitro* culture does not duplicate the intact state of the histological niche in which ADSCs are located (Jiang et al., 2023; Costa et al., 2021; Li et al., 2022). Therefore, we hypothesized that constructing an optimal culture model that both physiologically and physically reproduces *in situ* conditions to the greatest extent is urgently needed.

*In vivo* cell transplantation, a preclinical step in tissue engineering, is helpful for maintaining the characteristics of various groups of cells by providing the requisite environmentally relevant stimuli. The omentum and subcutaneous tissues of nude mice have been successfully used for culturing epithelial cells and chondrocytes, organs and tissues (Shuai et al., 2016; Suh et al., 2004; Buyukdogan et al., 2016; Zhou et al., 2016; Valerio, 2019; Mohamed et al., 2020). In such models, increased communication easily occurs between cells and surrounding components, thus leading to graft proliferation, angiogenesis and function (Suh et al., 2004; Buyukdogan et al., 2016; Zhou et al., 2016; Valerio, 2019; Mohamed et al., 2020). In addition, subcutaneously transplanted bone marrow MSCs have been shown to adapt well to the local microenvironment and to form multicellular aggregates that stimulate angiogenesis and mediate circulating cytokines (Mihai et al., 2020). These results jointly inspired us to explore whether *in vivo* transplantation culture could help ADSCs maintain or strengthen their intrinsic stemness.

Herein, by employing an animal transplantation model in the inguinal adipose tissues of nude mice, we investigated the stemness properties of ADSCs, including their proliferative ability, stemness-related marker expression, colony-forming efficiency, senescence, and multipotent differentiation capacity. Furthermore, a detailed transcriptome portrait of differentially cultured ADSCs and the possible underlying molecular mechanism were also generated. Our study may

facilitate *in vitro* ADSCs culture with improved properties and further guarantee optimized therapeutic effects.

## 2. Materials and methods

### 2.1. Animals

GFP-transgenic rats (female, 6–8 weeks, weighing 130–150 g) and nude mice (female, 6–8 weeks, weighing 20–25 g) were obtained from the Experimental Animal Center of Daping Hospital of Army Medical University (Chongqing, China). Animal care and procedures were approved by the Laboratory Animal Welfare and Ethics Committee of the Third Military Medical University (AMUWEC 20223443) and all animal experiments adhered to the relevant regulatory guidelines.

### 2.2. Isolation and culture of rat ADSCs

Subcutaneous inguinal adipose tissues were harvested from GFP-transgenic rats. GFP-positive ADSCs were isolated, cultured and identified according to our previous study (Wang et al., 2019). Briefly, the digested cells were resuspended in DMEM/F12 supplemented with 10 % fetal bovine serum (FBS) (Gibco, USA) and 1 % penicillin-streptomycin solution. ADSCs were incubated with culture medium at 37 °C in a humidified atmosphere containing 5 % CO<sub>2</sub>. The medium was changed every 2 days, and adherent cells were passaged at a ratio of 1:2 until they reached 80–90 % confluence with TrypLE Express solution (Gibco, USA). ADSCs at passage 4 were collected and divided into three groups for experiments.

### 2.3. In vivo transplantation and in vitro culture of rat ADSCs

One group of the 4th passage ADSCs was directly collected for further investigation (Con-ADSCs). The second group of 4th passage ADSCs was traditionally cultured and passaged in a cell incubator (Thermo, USA) (Vitro-ADSCs). The third group of ADSCs was resuspended in PBS at a concentration of  $1 \times 10^7$  cells/mL, and 100 µL of each cell suspension was injected into bilateral inguinal adipose tissues of nude mice that were intraperitoneally anesthetized with pentobarbital sodium using a microsyringe (Hamilton, Switzerland). Inguinal adipose tissues from nude mice were separated 3, 5 and 7 days after injection ( $n = 6$  mice/group). GFP-positive adipose tissues were subsequently selected under a fluorescence microscope, minced and digested with 0.075 % collagen II solution for 20 min at 37 °C. After neutralization and centrifugation, the pellets were plated onto culture dishes. The medium was changed every 24 h, and the cells were trypsinized and resuspended in PBS supplemented with 2 % FBS after 48 h of attachment. Fluorescence-activated cell sorting (FACS) (BD FACSAria™ II, USA) was used to collect GFP-positive ADSCs (Vivo-ADSCs). Vitro-ADSCs and Vivo-ADSCs were simultaneously collected for further investigation. The schematic illustration of our study is presented on Supplementary Fig. S1.

### 2.4. MTT assay

ADSCs were plated onto 96-well plates at a density of  $2 \times 10^3$  cells per well. Ten microliters of MTT solution (Solarbio, China) was added to the plates on Days 2, 4, 6, 8, 10 of attachment. After incubation at 37 °C for 4 h, the supernatants were discarded, and 150 µL of dimethyl sulfoxide was added. The OD values were measured at a wavelength of 490 nm using an ELISA reader (BioTek, USA).

### 2.5. Colony-forming unit (CFU) assay

The CFU assay was performed by plating  $1 \times 10^3$  ADSCs onto 10 cm plates, and maintaining the cells in growth medium every 4 days. After 14 days, the cells were fixed with 4 % paraformaldehyde (PFA) for 15 min and then stained with 3 % crystal violet solution (Beyotime,

China). Colonies with a cell number > 50 were counted under a microscope. Images of the cell stained with crystal violet were obtained with a scanner (Epson perfection V850 Pro, Japan).

## 2.6. Adipogenic, osteogenic and chondrogenic differentiation assays

To evaluate the differentiation abilities of ADSCs, all procedures were performed as previously reported (Wang et al., 2019). ADSCs collected from the three groups were plated onto 12-well plates at a density of  $3 \times 10^4$  per well and induced with the appropriate differentiation medium at 70–90 % confluence. After 15 days of adipogenic induction, lipid droplets and adipogenic-related genes were detected by Oil red O staining (Sigma, USA) and qRT–PCR, respectively. Calcium deposition was analyzed via Alizarin red S staining (Sigma, USA) and osteogenesis-associated genes were evaluated via qRT–PCR to detect osteogenic ability after 21 days of induction. For analysis of chondrogenic ability after 21 days of differentiation, sulfated glycosaminoglycan-rich extracellular matrix was detected by staining with Alcian blue solution (Sigma, USA) and chondrogenic-related gene was evaluated via qRT–PCR. Chemical staining images were obtained with a scanner (Epson perfection V850 Pro, Japan).

## 2.7. qRT–PCR

Total RNA was extracted with TRIzol reagent and reverse-transcribed using a Transcripter First Strand cDNA Synthesis Kit (Roche, Switzerland). Then, qRT–PCR was performed using FastStart Essential DNA Green Master Mix (Roche, Switzerland) on a LightCycler 96 detector (Roche, Switzerland). The expression levels of genes were analyzed and normalized to *Gapdh*. The fold changes in mRNA expression were evaluated using the  $2^{-\Delta\Delta CT}$  method. The primers used are listed in Supplementary Table 1.

## 2.8. Western blot analysis

ADSCs were lysed with RIPA buffer and centrifuged. Western blot analysis was performed as described previously (Wang et al., 2019). Briefly, the proteins were separated by SDS–PAGE and then transferred onto PVDF membranes after the BCA assay. The membranes were blocked with blocking solution (3 % w/v bovine serum albumin) and incubated with primary antibodies at room temperature for 1 h and at 4 °C overnight. Then, the membranes were incubated with horseradish peroxidase-conjugated secondary antibodies (Beyotime, China) at room temperature for 1 h and visualized by a VILBER Fusion FX6-XT Imaging System (VILBER, France) after washing. The following primary antibodies were used: anti-GAPDH (Beyotime AF1186, China), anti-NANOG (Abcam ab106465, UK), anti-OCT4 (Novus NB100-2379, USA), and anti-SOX2 (Bioworld AP0014, USA). GAPDH served as a loading control. Western blot images were analyzed using ImageJ.

## 2.9. Immunofluorescence

ADSCs were plated onto 48-well plates at a density of  $5 \times 10^3$  per well and allowed to attach overnight. The cells were fixed with 4 % PFA for 30 min, permeabilized with 0.1 % Triton X-100 for 10 min and blocked with 5 % BSA at room temperature for 1 h. The samples were then incubated with an anti-SOX2 antibody (1:200, Santa Cruz sc-365823, USA) overnight at 4 °C. After being washed with PBS, the ADSCs were incubated with an Alexa Fluor 555-conjugated secondary antibody (Beyotime A0460, China) for 2 h at room temperature in the dark. The nuclei were stained with DAPI, and images were acquired with a fluorescence microscope (Olympus, Japan).

## 2.10. RNA sequencing (RNA-seq) and bioinformatics analysis

Total RNA from ADSCs was used for RNA-seq analysis. Library

construction and sequencing were performed by OE Biotech (Shanghai, China) using the Illumina HiSeq X Ten platform. After quality assessment and postprocessing of the raw data, the sequences were mapped to the rat genome (RGSC Rnor\_6.0) using hisat2. Principal component analysis was used to analyze how individual samples related to each other based on the raw read counts of the conditions in R (v 3.2.0). Differentially expressed genes (DEGs) were identified using the DESeq (2012) R package functions estimate SizeFactors and nbinomTest. A *P* value < 0.05 and a fold change > 2 or < 0.5 were set as the thresholds for significantly differential expression. GO enrichment and KEGG pathway enrichment analyses of DEGs were performed using R based on the hypergeometric distribution.

## 2.11. Small interfering RNA (siRNA) transfection

siRNAs targeting *Egr1* or *Socs3*, nontargeting siRNA (siNC) and transfection reagents were obtained from Ribo (Guangzhou, China). Transfection complexes comprising siRNA, transfection buffer and transfection reagent were incubated at room temperature for 10 min and added to ADSCs. The medium was changed after 24 h. ADSCs were collected for RNA and protein analysis at 48 h and 72 h, respectively. The sequences of siRNAs used are listed in Supplementary Table 1.

## 2.12. Statistical analysis

All experiments were performed at least in triplicate, and the data are expressed as the mean ± SD. Student's *t* test was performed to analyze the differences between two groups, and one-way ANOVA was applied for analysis of differences among three groups, followed by a Bonferroni multiple comparison post hoc test using GraphPad Prism software v 5.04. \**P* < 0.05 represents statistical significance.

## 3. Results

### 3.1. In vivo culture conditions maintained the morphology of ADSCs

Con-ADSCs exhibited a fibroblast-like morphology, were spindle-shaped and poly-shaped, and stably expressed GFP (Fig. 1A). Then, the Con-ADSCs were cultured under *in vivo* and *in vitro* conditions. Microscopic photos were captured on Day 3, Day 5 and Day 7. GFP-positive ADSCs in separated and minced inguinal adipose tissues of nude mice exhibited a three-dimensional growth pattern with pseudopodia, and maintained growth pattern and morphology with increasing time (Fig. 1B). After attachment to dishes for 24 h, Vivo-ADSCs exhibited spindle and polygonal shapes with relatively high dipters and maintained morphologies with smooth cell surfaces at all given time points (Fig. 1B). In contrast, a greater proportion of cells with a senescent phenotype (flat-shaped morphologies with lower dipters) was observed among the Vitro-ADSCs at the corresponding time points and as the expansion time progressed (Fig. 1B). However, the number of Vivo-ADSCs decreased with prolonged culture time (Fig. 1B and Fig. S2).

### 3.2. In vivo culture conditions improved the expression of stemness-related markers in ADSCs

*Nanog*, *Oct4* and *Sox2* are the main transcription factors involved in regulating the stemness properties of ADSCs (Zhou et al., 2021; Rangasami et al., 2021). The effects of different culture conditions on stemness-related marker expression were evaluated at both mRNA and protein levels. qRT–PCR data revealed no significant differences in *Nanog*, *Oct4* or *Sox2* expression levels between Vivo-ADSCs and Vitro-ADSCs until Day 5 or Day 7 (Fig. 2A–C). Similarly, the protein expression levels of these markers were upregulated in Vivo-ADSCs compared to those in Vitro-ADSCs at Days 5 and 7. Moreover, ADSCs subjected to serial passaging in an incubator exhibited decreased *NANOG*, *OCT4* and *SOX2* expression levels (Fig. 2D–I).

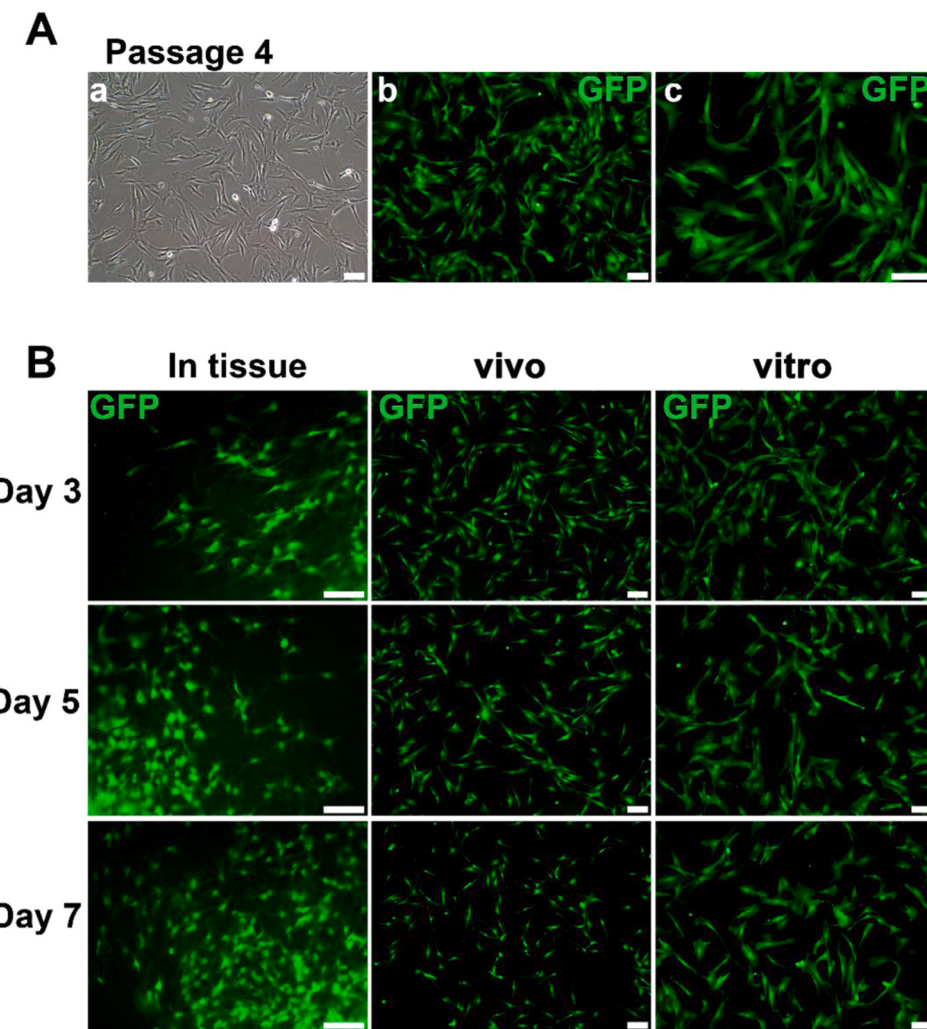


**Fig. 1.** Cell morphology of ADSCs. (A) Representative phase-contrast image (a) and fluorescence image (b, c) of Con-ADSCs. (B) Representative fluorescence microscopic morphology of Vitro-ADSCs and Vivo-ADSCs at 3 days, 5 days and 7 days. Left panel: ADSCs in minced inguinal adipose tissues of nude mice; middle panel: Vivo-ADSCs were reisolated and plated on dishes for 24 h; right panel: Vitro-ADSCs. Scale bar: 100  $\mu$ m; magnification: 100 $\times$ .

Immunofluorescence results further confirmed that Vitro-ADSCs exhibited a reduced SOX2 expression level with long-term expansion and that Vivo-ADSCs exhibited an increased SOX2 expression level (Fig. 2J).

### 3.3. In vivo culture conditions enhanced the proliferation and reduced the senescence of ADSCs

The proliferation of ADSCs was evaluated by MTT and CFU assays. MTT results indicated that Vivo-ADSCs had greater proliferative ability than Vitro-ADSCs on Days 3, 5 and 7 (Fig. 3A–C). CFUs assay further exhibited that colonies generated by Vivo-ADSCs significantly outnumbered those generated by Vitro-ADSCs both on Day 5 and Day 7, but were less than those generated by Con-ADSCs at each time point (Fig. 3D–E). Additionally, the senescence markers *p21* and *p15* were evaluated at the transcriptional level by qRT–PCR. The results showed that *p21* and *p15* levels were significantly elevated in Vitro-ADSCs compared with those in Vivo-ADSCs and Con-ADSCs at all given time points (Fig. 3F–H).

### 3.4. In vivo culture conditions increased the adipogenic differentiation capacity of ADSCs

One essential property of ADSCs is that they can differentiate into

mesoderm-derived cells (especially adipocytes, osteoblasts and chondrocytes), which is currently considered a key part of stemness evaluation (Zhou et al., 2021; Bacakova et al., 2018). To determine the adipogenic differentiation ability of ADSCs, cells were induced in adipogenic medium for 15 days. qRT–PCR data revealed no significant differences in the expression of adipogenic genes (*Fabp4*, *Lpl* and *Ppar- $\gamma$* ) between Vivo-ADSCs and Vitro-ADSCs on Days 3 and 5. Moreover, the Con-ADSCs had greater adipogenic ability than did the other two groups on Day 5 (Fig. 4A–B). On Day 7, adipogenic gene expression in Vivo-ADSCs was significantly higher than that in Vitro-ADSCs but lower than that in Con-ADSCs (Fig. 4C). Analysis of Oil red O staining confirmed that the proportions of round lipid droplets in Vivo-ADSCs and Vitro-ADSCs were basically in accordance with the gene results (Fig. 4D).

### 3.5. In vivo culture conditions increased the osteogenic differentiation potential of ADSCs

ADSCs induced in osteogenic medium for 21 days were collected for qRT–PCR analysis and Alizarin red S staining. The results indicated a similar degree of calcium deposition in Vivo-ADSCs and Vitro-ADSCs on Day 3 (Fig. 5A). However, the expression levels of osteogenic markers (*Alp* and *Runx2*) were higher in the Vivo-ADSCs than in the Vitro-ADSCs (Fig. 5D). Prolonged culture time *in vivo* increased the mineralization

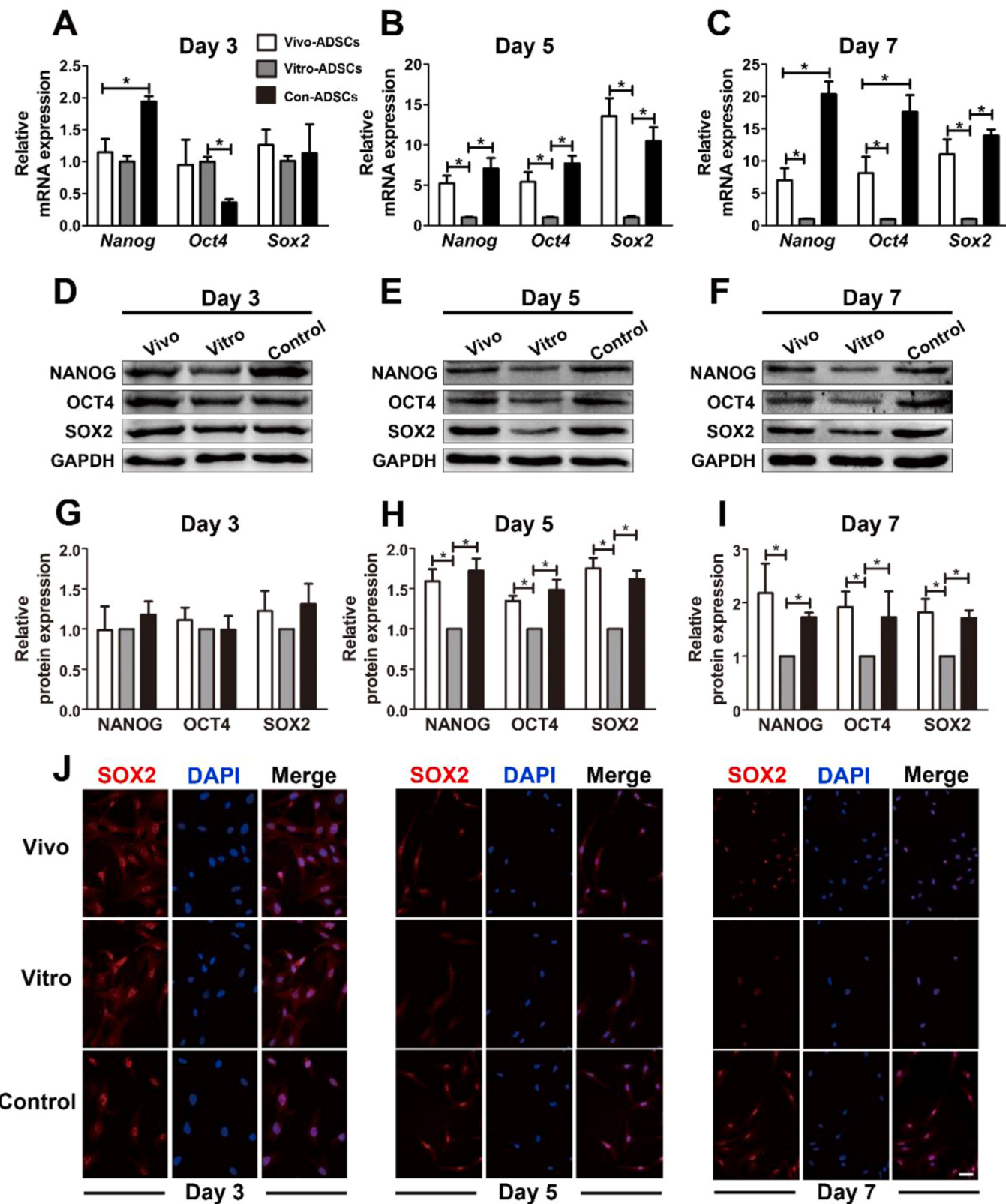


**Fig. 2.** Expression of stemness-related markers in ADSCs. (A–C) The mRNA levels of *Nanog*, *Oct4* and *Sox2* were measured by qRT–PCR. The results were normalized against *Gapdh* ( $n = 3$ ). (D–I) *NANOG*, *OCT4* and *SOX2* protein levels were analyzed via Western blotting. GAPDH was used as a loading control. Representative blots of different groups at Days 3 (D), 5 (E) and 7 (F). Quantitative measurements of the protein levels (G–I) ( $n = 3$ ); the protein expression levels in *Vitro*-ADSCs were taken as 1.0. (J) Representative images of *SOX2* expression evaluated by immunofluorescence. Red fluorescence (Alexa Fluor 555): *SOX2*; blue fluorescence: DAPI. Scale bar: 50  $\mu$ m; magnification: 200  $\times$ , \*  $P < 0.05$ .

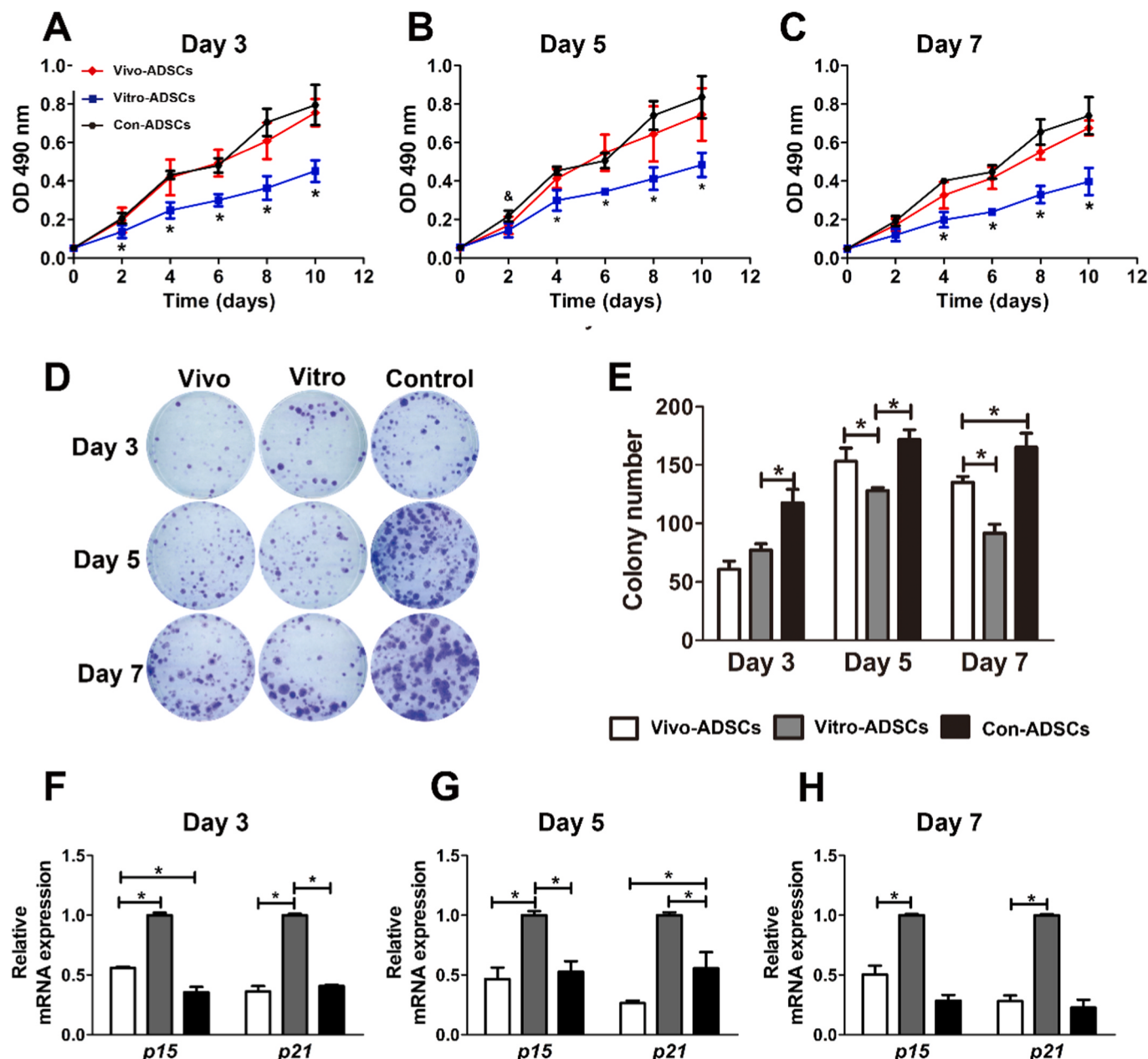


**Fig. 3.** Proliferative ability and senescence of ADSCs. (A–C) Con-ADSCs, Vivo-ADSCs and Vitro-ADSCs were seeded onto 96-well plates, and an MTT assay was used to examine their proliferation ability. \*  $P < 0.05$  compared with Vivo-ADSCs and Con-ADSCs, &  $P < 0.05$  compared with Vivo-ADSCs. (D–E) Colony-forming efficiency of ADSCs. Representative images of colonies stained with crystal violet (D); the number of colonies containing more than 50 cells was counted (E) ( $n = 3$ ). (F–H) qRT–PCR analysis of *p15* and *p21* mRNA expression in ADSCs. The results were normalized against *Gapdh* ( $n = 3$ ). \*  $P < 0.05$ .

potential of Vivo-ADSCs compared with that of Vitro-ADSCs (Fig. 5B–C). At the mRNA level, Vivo-ADSCs showed upregulated expression levels of *Alp* and *Runx2* compared with those in Vitro-ADSCs after induction, while the expression of another osteogenic marker, *Bsp*, in Vivo-ADSCs increased only on Day 7 (Fig. 5E–F).

### 3.6. In vivo culture conditions increased the chondrogenic differentiation ability of ADSCs

Differences in the chondrogenic capacity of ADSCs were further analyzed. Alcian blue staining revealed a greater number of positive cells in Vivo-ADSCs than in Vitro-ADSCs at Days 3, 5 and 7 (Fig. 6A). Next, we measured aggrecan expression (a chondrogenic marker) by qRT–PCR analysis. Similarly, the data indicated that Vivo-ADSCs had higher aggrecan expression level than Vitro-ADSCs after chondrogenic

induction (Fig. 6B–D).

### 3.7. In vivo culture conditions altered the gene expression profiles of ADSCs

The aforementioned results demonstrated that, compared with those of Vitro-ADSCs, Vivo-ADSCs exhibited enhanced stemness properties on Day 7. Therefore, we compared the transcriptome features of these two groups of cells and Con-ADSCs. RNA-seq data revealed that 419 DEGs were detected in Vitro-ADSCs compared with those in Con-ADSCs and 1308 DEGs between Vivo-ADSCs and Vitro-ADSCs. Among the DEGs, 220 genes were commonly shared (Fig. 7A–C and Fig. S2). The details of the GO and KEGG pathway analyses of these DEGs are provided in the supplementary files (Fig. S3, 4). Briefly, GO analysis showed that the DEGs were mainly related to the regulation of cell proliferation, gene

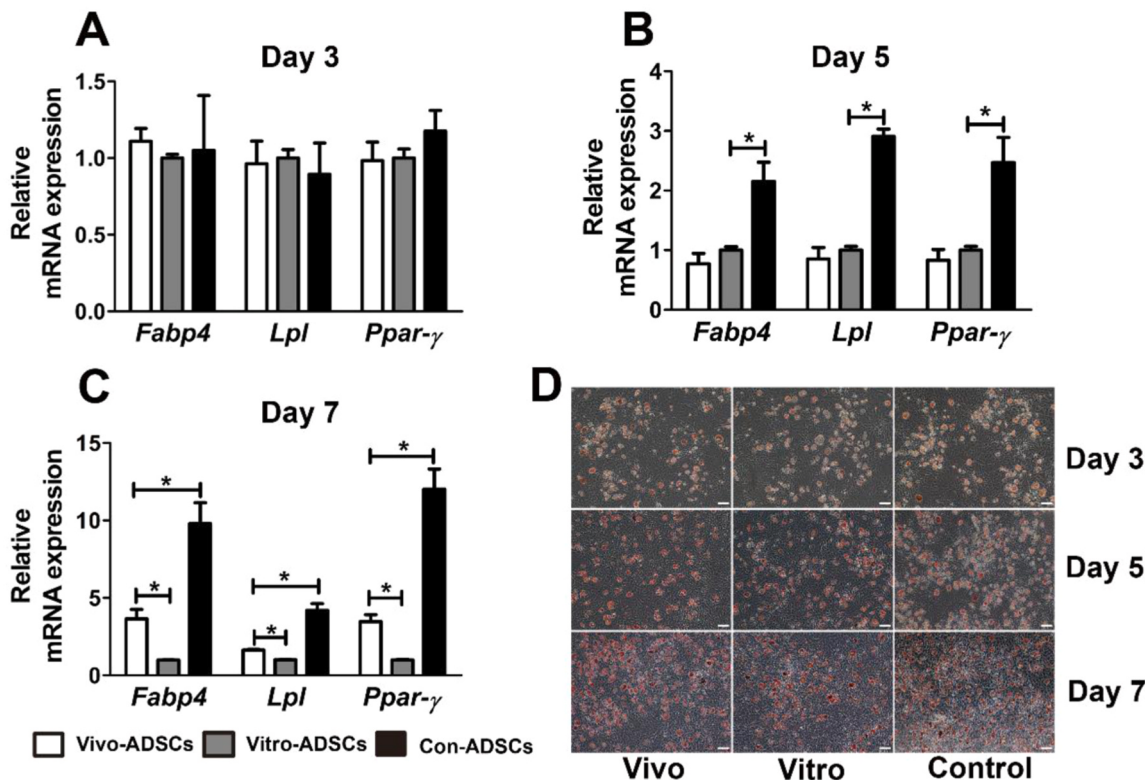


**Fig. 4.** Adipogenic differentiation capacity of ADSCs. (A–C) ADSCs were induced in adipogenic medium for 15 days, and the expression of adipogenic markers (*Fabp4*, *Lpl* and *Ppar-γ*) was measured by qRT–PCR. The results were normalized against *Gapdh* ( $n = 3$ ). \*  $P < 0.05$ . (D) Oil red O staining was further used to detect lipid droplets in the cytoplasm of ADSCs after 15 days of induction. Scale bar: 100  $\mu$ m; magnification: 100  $\times$ .

expression, transcription, and extracellular matrix organization. KEGG analysis revealed that the DEGs were mostly enriched in pathways such as cytokine–cytokine receptor interaction pathways, Notch, JAK–STAT and signaling pathways regulating the pluripotency of stem cells (Fig. 7D, E and Fig. S4). Finally, qRT–PCR results further revealed that 8 selected genes exhibited similar expression patterns to the RNA-seq data, indicating the reliability of these data (Fig. 7F–G and Fig. S5).

### 3.8. *Egr1* regulated stemness-related markers in ADSCs

Based on the results of bioinformatics analyses, we hypothesized that increased communication between ADSCs and the surrounding microenvironment stimulated by a variety of signaling pathways may have occurred during the *in vivo* culture course. Notably, we observed changes in *Egr1* and *Socs3* in ADSCs. *Egr1* has been identified as a transcription factor that contributes to cell proliferation, differentiation and secretion when stimulated by the surrounding environment. *Socs3* is an inhibitor of the cytokine-JAK-STAT signaling pathway and a key regulator of cell functions (Zhang et al., 2019; Tamama and Barbeau, 2012). Herein, to explore the effects of these two genes on stemness regulation, we downregulated the expression of *Egr1* and *Socs3* in Vitro-ADSCs by siRNA (Fig. S6). The results indicated that significantly decreased *Nanog*, *Oct4* and *Sox2* expression levels were observed only in the *Egr1* interference group (Fig. 8 A–C). Similarly, the protein levels of NANOG, OCT4 and SOX2 were reduced when *Egr1* was downregulated in ADSCs, and these changes were not observed in the *Socs3* interference group (Fig. 8 D, E). These findings indicated that *Egr1* might positively regulate stemness-related marker expression in ADSCs.

## 4. Discussion

Current preclinical experiments and clinical trials have shown that

the robust therapeutic efficacy of MSCs strongly depends on their stemness properties and multiple-dosing regimens (Zhou et al., 2021; Bacakova et al., 2018; Fazekas et al., 2022; Gong et al., 2022; Song et al., 2018; Armin et al., 2023). During *in vitro* expansion of MSCs, cell stemness inevitably declines with cell passaging (Shuai et al., 2016; He et al., 2024; Wang et al., 2021). Therefore, obtaining a high quantity of MSCs while maintaining their good stemness poses an urgent challenge. In this study, we adopted inguinal adipose tissues as an “incubator” to provide a physiologically and physically simulating niche for ADSCs. Our findings showed that ADSCs transplanted into adipose tissues maintained their stemness properties via various mechanisms, including changes in various genes and signaling pathways. Specifically, an *Egr1*-containing signaling pathway may participate. These results provide potential intervening strategies for improving stemness properties of expanding ADSCs within laboratory condition and further strengthen therapeutic effects.

Cell transplantation has been reported to suffer from limitations such as difficult cell tracing and a low survival rate (Zhuang et al., 2021; Ma et al., 2018; Liu et al., 2012). Persistent expression of enhanced GFP in cells is known to be advantageous for detecting and monitoring graft distribution, growth and differentiation *via* fluorescence imaging (Ahn et al., 2008; Kircher et al., 2011). In this study, ADSCs obtained from GFP transgenic rats consistently expressed GFP and were easily sorted by high-purity flow cytometry. As shown by the microscopic and FACS results, the number of transplanted ADSCs decreased with prolonged culture time, and only 12 % of the initial ADSCs were sorted one week after injection. As reported, transplanted cells in the body may undoubtedly die due to harsh changes in the original niche, such as hypoxia, oxidative stress and inflammation (Li et al., 2022; Ma et al., 2018; Liu et al., 2012; Meyerrose et al., 2007). In addition, once stem cells are administered to the body, their deformability and migratory ability allow them to be distributed throughout the body rather than remaining

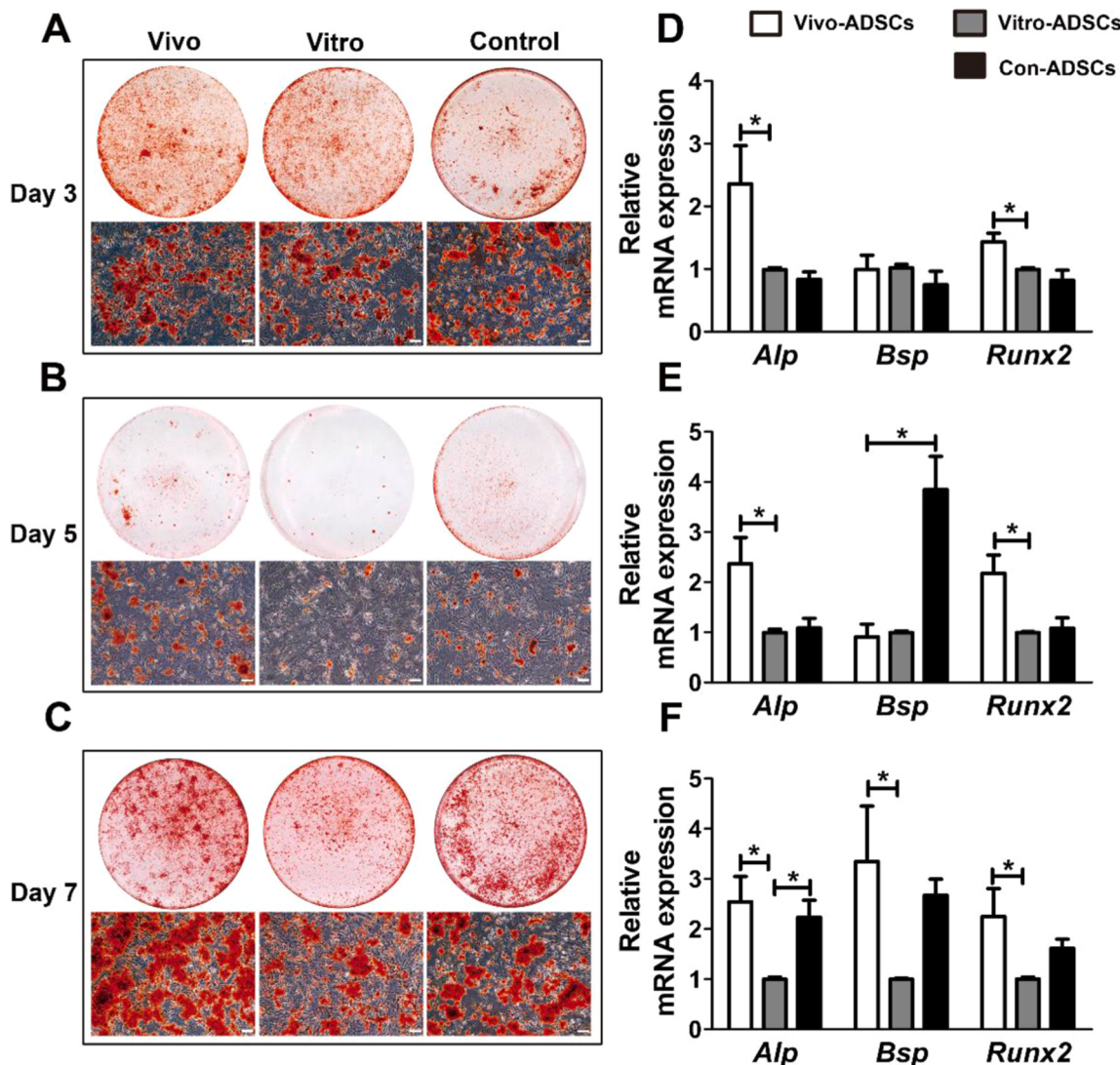


**Fig. 5.** Osteogenic differentiation ability of ADSCs. Con-ADSCs, Vivo-ADSCs and Vitro-ADSCs were cultured in osteogenic induction medium for 21 days. (A–C) Representative images of calcium nodule deposition in ADSCs stained with Alizarin red S. Scale bar: 100  $\mu$ m; magnification: 100  $\times$ . (D–F) The mRNA levels of osteogenic markers (*Alp*, *Bsp* and *Runx2*) were measured by qRT–PCR. The results were normalized against *Gapdh* ( $n = 3$ ). \*  $P < 0.05$ .

at the injection site (Liu et al., 2012; Meyerrose et al., 2007; Moya et al., 2018). In light of the above findings, a significant reduction in cell numbers occurred during *in vivo* transplantation, but the stemness properties of *in vivo* cultured ADSCs were maintained in our study, thereby supporting the application of this model as an ADSC culture strategy.

Maintaining morphology and vigorous proliferation are challenging issues during the expansion process. These biological features commonly negatively change with extensive culture *in vitro*, which could be interpreted as cellular senescence, characterized by increased expression of p15 and p21 (Weng et al., 2022; Oh et al., 2014; Li et al., 2019; Yew et al., 2011). Our results indicated that *in vitro* culture decreased the growth rate and accelerated the senescence of ADSCs, while transplanted ADSCs in inguinal adipose tissues showed active proliferation and minor senescence, similar to cells at earlier passages. These results agree with previous studies showing that optimized protocols that simulate a more relevant *in situ* niche benefit stemness maintenance (Shuai et al., 2016; Di et al., 2021). Additionally, the stemness-related markers Nanog, Oct4 and Sox2 play pivotal roles in maintaining the self-renewal and differentiation capabilities of ADSCs (Zhou et al., 2021; Jiang et al., 2023; Rangasami et al., 2021; Tsai et al.,

2012; Han et al., 2014). *In vitro* expansion of ADSCs under hypoxia, spheroid culture and the presence of necessary factors can upregulate the expression of these markers and improve self-renewal and multi-lineage differentiation abilities, thereby increasing therapeutic efficacy (Cao et al., 2020; Qiao et al., 2020; Liu et al., 2021). Moreover, the upregulation of stemness-related markers by gene manipulation also has similar effects (Zhou et al., 2021; Jiang et al., 2023; Han et al., 2014; Shi et al., 2017). In this study, ADSCs cultured *in vivo* exhibited higher levels of stemness-related markers than did incubator-cultured ADSCs, suggesting that our optimized culture method may facilitate stemness maintenance by regulating stemness-related marker expression. It seems that enhanced expression of stemness-related markers may indicate better plasticity of ADSCs (Zhou et al., 2021). However, our study revealed that the changes in the adipogenic differentiation of ADSCs on Day 5 were not in line with the variations in the levels of multiple potent markers. To our knowledge, the average doubling time of ADSCs varies from 36 to 72 h, and the time of significant property changes may vary with different conditions (Shuai et al., 2016; Arrigoni et al., 2009; Ohta et al., 2018). Data from Flynn et al. demonstrated that adipose-derived ECM exhibits compositional and biomechanical properties that induce adipogenesis (Yu et al., 2017), who used decellularized adipose tissue

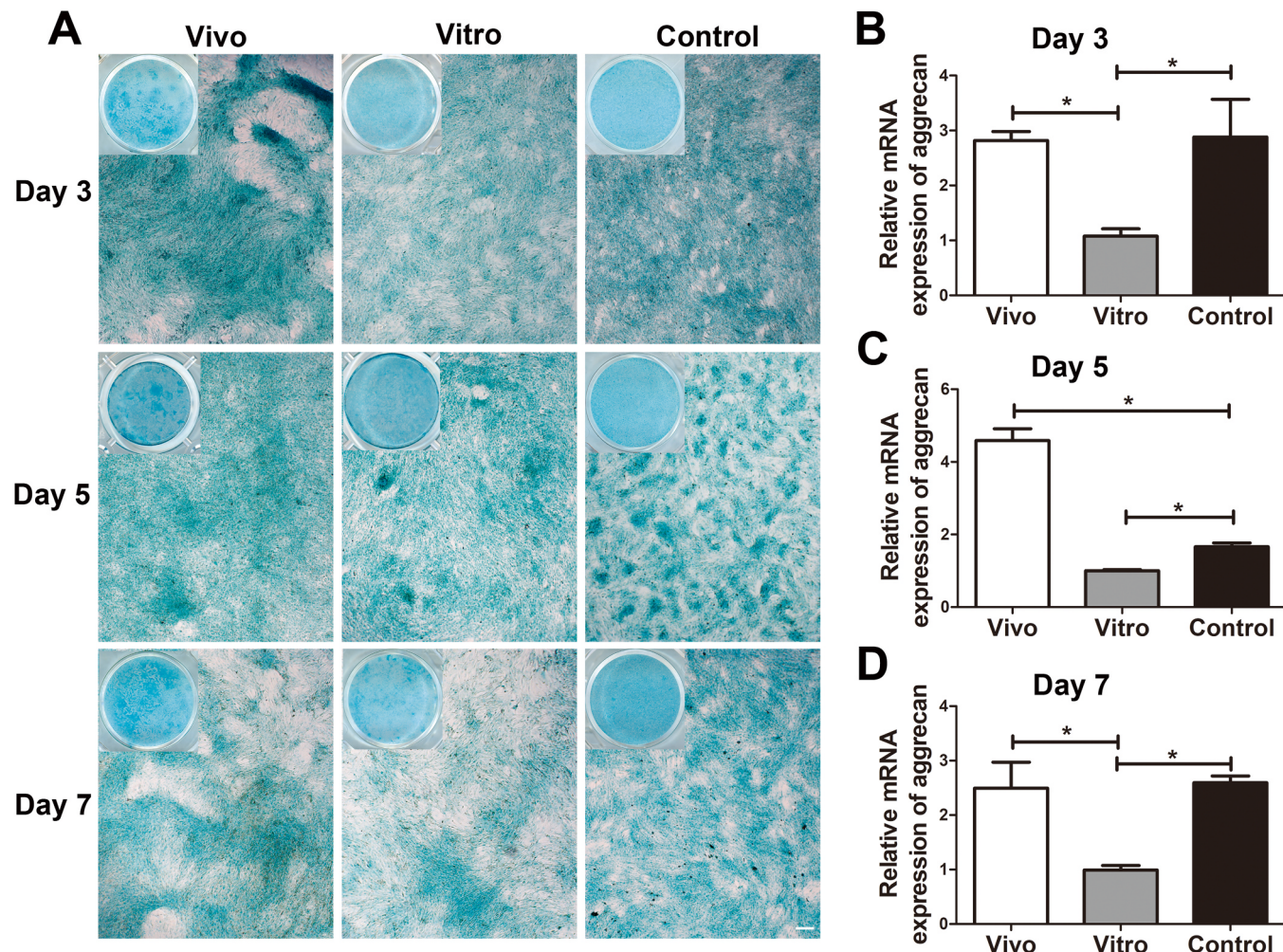


**Fig. 6.** Chondrogenic differentiation capacity of ADSCs. Con-ADSCs, Vivo-ADSCs and Vitro-ADSCs were induced in chondrogenic medium for 21 days. (A) Acid proteoglycans were measured by Alcian blue staining. Scale bar: 200  $\mu$ m; magnification: 40  $\times$ . (B–D) The expression levels of the chondrogenic marker aggrecan in ADSCs determined by qRT–PCR. The results were normalized against *Gapdh* ( $n = 3$ ). \*  $P < 0.05$ .

microcarriers as an ADSC culture model. Therefore, we speculate that ADSCs cultured in adipose tissues are possibly induced by the ECM, tend to undergo adipogenic differentiation, and maintain multilineage differentiation ability.

The microenvironment determines stem cell fate and maintains ADSC homeostasis. The components of niches and their interactions are complicated (Scadden, 2006; Jiang et al., 2023). Our RNA-seq data indicated that most DEGs were located in the extracellular space, membrane and ECM, in connection with functions such as protein binding and transcription regulation. Soluble proteins (e.g., growth factors, chemokines, nutrients) in the stem cell niche improve cell-cell or cell-acellular element interactions and regulate gene transcription, further controlling stemness properties by binding to their receptors (Zhou et al., 2021; Scadden, 2006). We found that the expression of cytokines and cytokine receptors, such as *Lifr*, *Igf1* and *Igfbp4*, was increased in *in vivo* cultured ADSCs. These genes have been demonstrated to be closely related to stemness properties in recent studies (Liang et al., 2022; Youssef et al., 2017; Chen et al., 2020; Maridas et al., 2017). ECM, as a reservoir of secretory factors, not only transmits biochemical signals but also delivers physical information such as that from matrix hardness and topography (Niklason, 2018). Growth factors in the ECM are blocked by certain proteins. Improving their functions could be achieved by degradation or recombination of the ECM (Tratwal et al., 2015). According to the RNA-seq data, genes that degrade or recombine ECM (e.g., *Mmp2*, *Mmp3* and *Adamts15*) were upregulated in

*in vivo* cultured ADSCs. In addition, the Notch signaling pathway is involved in stemness maintenance, and *Jag1* reportedly improves communication between stem cells and their surroundings (Pagella et al., 2021; Bigas and Porcheri, 2018). Both signaling pathways were increased in *in vivo* cultured ADSCs. Therefore, these results suggest that *in vivo* culture conditions regulating the properties of ADSCs might be achieved by facilitating the secretion of ADSCs and subsequently enhancing cell-cell or cell-ECM contacts.

Cell-to-microenvironment interactions may trigger multiple intracellular signaling pathways and subsequently control the expression of various genes and proteins. *Egr1*, an early activated factor involved in the process of cellular responses to environmental stimuli, has been shown to regulate stem cell proliferation, differentiation and secretion (Tamama and Barbeau, 2012; Qiu et al., 2019; Li et al., 2020). In the present study, *in vivo* cultured ADSCs exhibited more primitive stemness properties and increased *Egr1* expression, suggesting that *Egr1* might be involved in this process. As a transcription factor, *Egr1* can be activated by a number of signaling pathway factors (e.g., *Mapk*, *Erk*, *Dusp* and *Jak*) and subsequently triggers alterations in many downstream genes, such as *Lif*, *p15* and *p21* (Tamama and Barbeau, 2012; Li et al., 2019; Baek et al., 2022; Yang et al., 2019). Our KEGG analysis also revealed that the signaling pathways regulating the pluripotency of stem cells and the JAK-STAT pathway were increased in *in vivo* cultured ADSCs. These signaling pathways included elevated *Mapk*, *Jak*, and *Lifr* levels, indicating that *Egr1* may serve as a downstream mediator. Furthermore, we

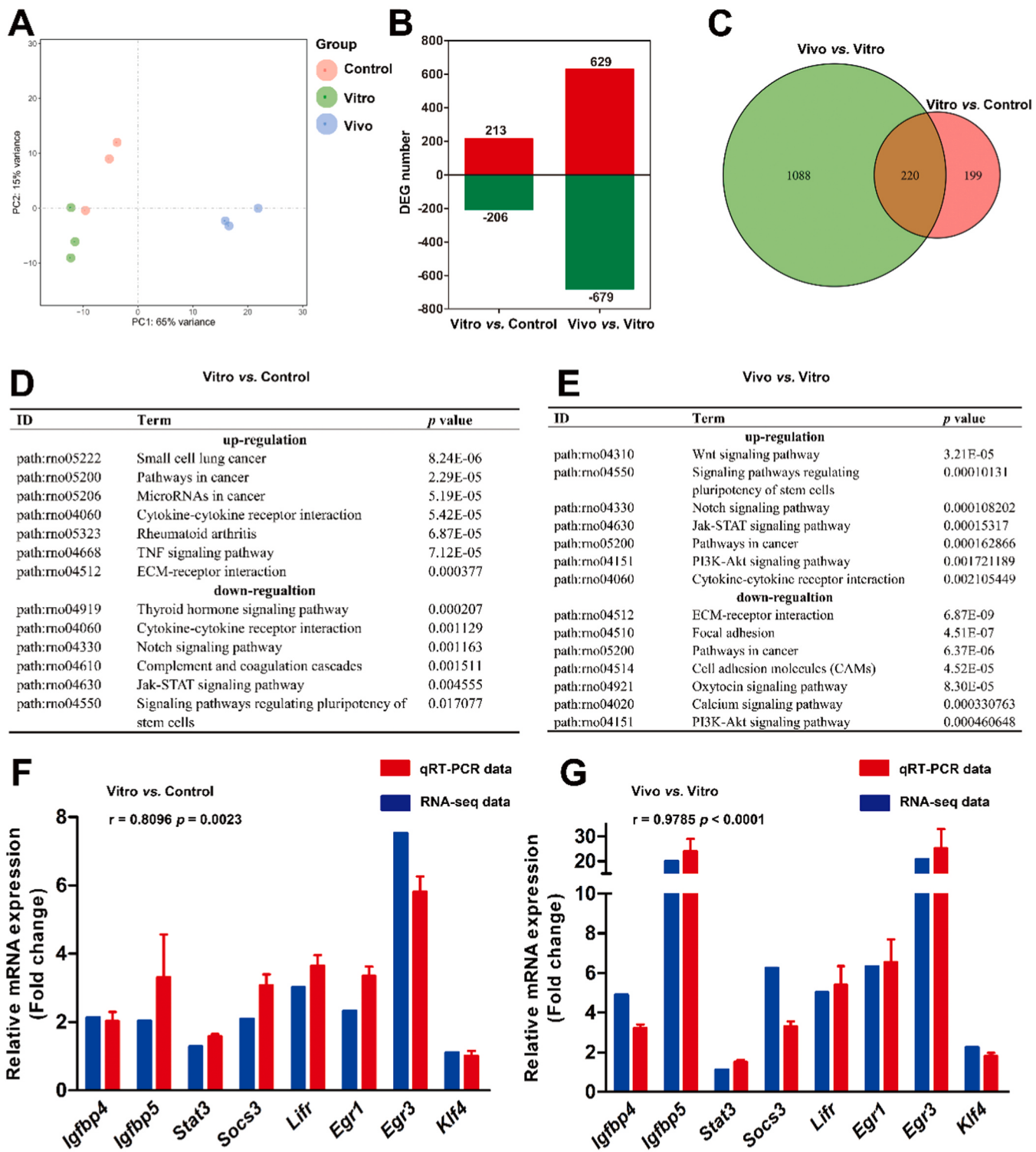


**Fig. 7.** Gene expression profiles of ADSCs. (A) Principal component analysis (PCA) of the DEGs. (B) Bar plot illustrating up- and downregulated genes from the two comparison datasets (Vitro-ADSCs vs. Con-ADSCs and Vivo-ADSCs vs. Vitro-ADSCs). (C) Venn diagram of the DEGs. (D–E) Main KEGG analysis of highly enriched pathways for up- and downregulated genes in Vitro-ADSCs vs. Con-ADSCs (D) and in Vivo-ADSCs vs. Vitro-ADSCs (E). (F–G) Validation of RNA-seq through qRT-PCR. Fold changes of 8 selected genes expression from Vitro-ADSCs vs. Con-ADSCs (F) and from Vivo-ADSCs vs. Vitro-ADSCs (G). Pearson correlation coefficient ( $r$ ) and  $p$  value are reported. For qRT-PCR analysis, the results were normalized against *Gapdh* ( $n = 3$ ).

found that downregulation of *Egr1* resulted in decreased levels of stemness-related markers. Therefore, we propose that an *Egr1*-involved signaling pathway may restore the stemness properties of ADSCs cultured in adipose tissues by targeting stemness-related markers.

However, additional mechanisms need to be elucidated in the future.

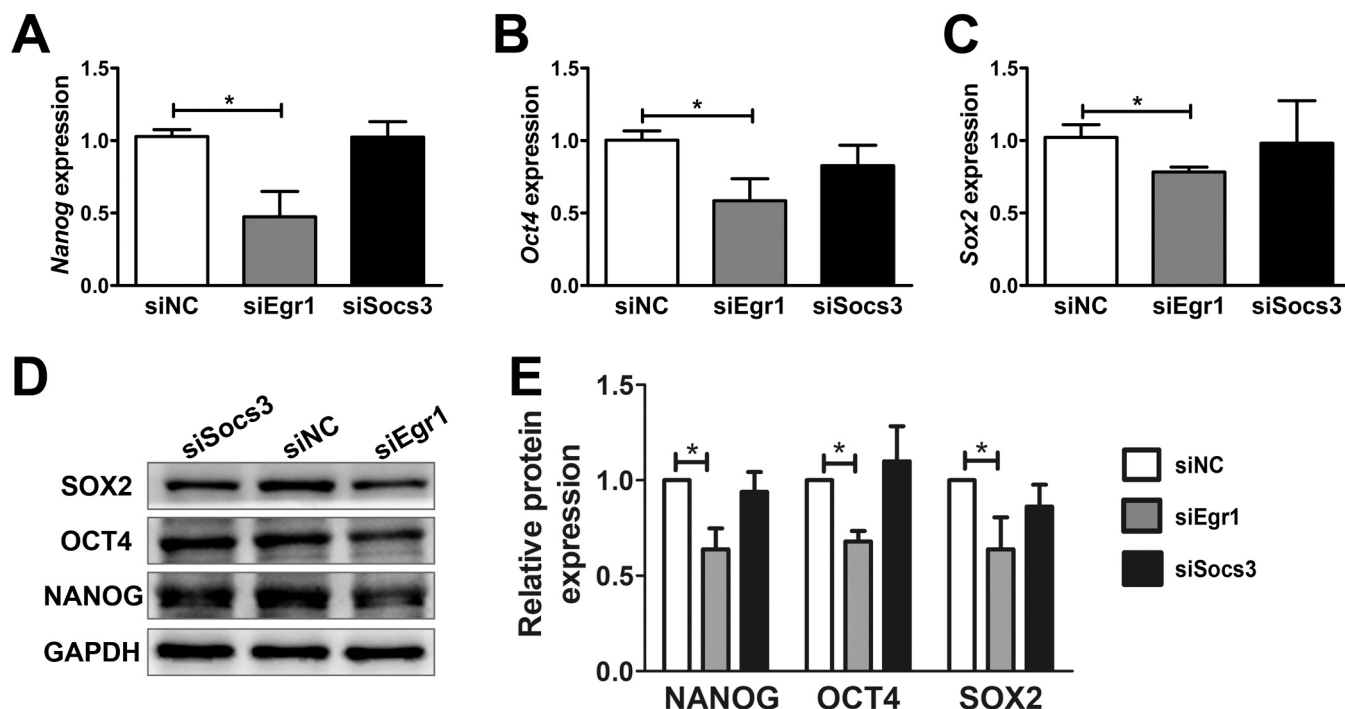


**Fig. 8.** Stemness-related marker expression in ADSCs after Egr1 and Soc3 interference. *In vitro* cultured ADSCs were transfected with siRNA or control siRNA (siNC) and then collected for mRNA and protein analyses. (A–C) qRT–PCR analysis of stemness-related marker expression levels. The results were normalized against *Gapdh* ( $n = 3$ ). \*  $P < 0.05$ . (D) Western blot images of stemness-related marker expression in ADSCs and (E) the quantitative analysis of the protein levels ( $n = 3$ ). GAPDH was used as a loading control. The protein levels in the siNC group were set as 1. \*  $P < 0.05$ .

## 5. Conclusion

In summary, we reported that *in vivo* culture conditions involving the transplantation of separated ADSCs to *in situ* adipose tissues could enhance the stemness properties of ADSCs. We further revealed that transplanted ADSCs exhibited considerable crosstalk at the transcriptional level and that an Egr1-related signaling pathway might contribute to maintaining stemness. This study provides important insights into effective strategies to enhance the stemness properties of ADSCs for extensive clinical application.

## Authors' contributions

Xu Feng and Bo Zhang designed the study and analyzed the data. Chao Wang and Tian Xie participated in the animal experiments and prepared the manuscript. Chao Wang, Tian Xie, Xue Lu, Changxue Xiao and Xiaoming Li participated in the isolation and culture of ADSCs and molecular biology analysis. Ping Liu and Feng Xu provided assistance in the design of the study and data gathering. All authors have read and approved the final manuscript.

## Funding

This work was financially supported by the Youth Basic Research Project from the Ministry of Education Key Laboratory of Child Development and Disorders (No. YBRP-202118).

## CRediT authorship contribution statement

**Bo Zhang:** Writing – review & editing, Supervision, Project administration, Funding acquisition, Conceptualization. **Feng Xu:** Supervision, Resources, Project administration, Funding acquisition, Conceptualization. **Xue Lu:** Visualization, Validation, Methodology, Data curation. **Xiaoming Li:** Writing – review & editing, Validation, Methodology, Formal analysis. **Ping Liu:** Resources, Project

administration. **changxue Xiao:** Validation, Methodology, Data curation. **Tian Xie:** Writing – review & editing, Writing – original draft, Visualization, Validation, Methodology. **Chao Wang:** Writing – original draft, Validation, Methodology, Funding acquisition, Data curation, Conceptualization.

## Declaration of Competing Interest

The authors declare no competing interests.

## Data availability statement

The datasets used and/or analyzed during the current study are available from the corresponding author upon reasonable request. The RNA-seq data can be found in the GEO repository and are accessible under the series accession number [GSE261680](#).

## Acknowledgments

Not applicable.

## Appendix A. Supporting information

Supplementary data associated with this article can be found in the online version at [doi:10.1016/j.mad.2024.111935](#).

## References

- Ahn, K.S., Jeon, S.J., Jung, J.Y., et al., 2008. Isolation of embryonic stem cells from enhanced green fluorescent protein-transgenic mouse and their survival in the cochlea after allotransplantation. *Cyotherapy* 10 (7), 759–769.
- Armin, A., Mohsen, F.K., Kamran, H., et al., 2023. Effect of once versus twice intracoronary injection of allogeneic-derived mesenchymal stromal cells after acute myocardial infarction: BOOSTER-TAHAT randomized clinical trial. *Stem Cell Res. Ther.* 14 (1), 264.

- Arrigoni, E., Lopa, S., de Girolamo, L., Stanco, D., Brini, A.T., 2009. Isolation, characterization and osteogenic differentiation of adipose-derived stem cells: from small to large animal models. *Cell Tissue Res.* 338 (3), 401–411.
- Bacakova, L., Zarubova, J., Travnickova, M., et al., 2018. Stem cells: their source, potency and use in regenerative therapies with focus on adipose-derived stem cells – a review. *Biotechnol. Adv.* 36 (4), 1111–1126.
- Baek, J., Lopez, P.A., Lee, S., Kim, T.S., Kumar, S., Schaffer, D.V., 2022. Egr1 is a 3D matrix-specific mediator of mechanosensitive stem cell lineage commitment. *Sci. Adv.* 8 (15), eabm4646.
- Bigas, A., Porcheri, C., 2018. Notch and stem cells. *Adv. Exp. Med. Biol.* 1066, 235–263.
- Buyukdogan, K., Doral, M.N., Bilge, O., Turhan, E., Huri, G., Sargon, M.F., 2016. Peritoneum and omentum are natural reservoirs for chondrocytes of osteochondral autografts: a comparative animal study. *Acta Orthop. Trauma. Turc.* 50 (5), 539–543.
- Cao, Z., Xie, Y., Yu, L., Li, Y., Wang, Y., 2020. Hepatocyte growth factor (HGF) and stem cell factor (SCF) maintained the stemness of human bone marrow mesenchymal stem cells (hBMSCs) during long-term expansion by preserving mitochondrial function via the PI3K/AKT, ERK1/2, and STAT3 signaling pathways. *Stem Cell Res. Ther.* 11 (1), 329.
- Chen, P.C., Kuo, Y.C., Chuong, C.M., Huang, Y.H., 2020. Niche modulation of IGF-1R signaling: its role in stem cell pluripotency, cancer reprogramming, and therapeutic applications. *Front. Cell Dev. Biol.* 8, 625943.
- Costa, L.A., Eiro, N., Fraile, M., et al., 2021. Functional heterogeneity of mesenchymal stem cells from natural niches to culture conditions: implications for further clinical uses. *Cell. Mol. Life Sci.* 78 (2), 447–467.
- Di, S.A.B., Grisafi, F., Perez-Alca, M., et al., 2021. Cell quality evaluation with gene expression analysis of spheroids (3D) and adherent (2D) adipose stem cells. *Gene* 768, 145269.
- Fazekas, B., Alagesan, S., Watson, L., et al., 2022. Comparison of single and repeated dosing of anti-inflammatory human umbilical cord mesenchymal stromal cells in a mouse model of polymicrobial sepsis. *Stem Cell Rev. Rep.* 18 (4), 1444–1460.
- Gong, C., Chang, L., Sun, X., et al., 2022. Infusion of two-dose mesenchymal stem cells is more effective than a single dose in a dilated cardiomyopathy rat model by upregulating indoleamine 2,3-dioxygenase expression. *Stem Cell Res. Ther.* 13 (1), 409.
- Han, S.M., Han, S.H., Coh, Y.R., et al., 2014. Enhanced proliferation and differentiation of Oct4- and Sox2-overexpressing human adipose tissue mesenchymal stem cells. *Exp. Mol. Med.* 46, e101.
- He, L., Li, M., Wang, X., et al., 2024. Morphology-based deep learning enables accurate detection of senescence in mesenchymal stem cell cultures. *BMC Biol.* 22 (1), 1.
- Hu, C., Li, L., 2018. Preconditioning influences mesenchymal stem cell properties in vitro and in vivo. *J. Cell. Mol. Med.* 22 (3), 1428–1442.
- Ichikado, K., Kotani, T., Kondoh, Y., et al., 2023. Clinical efficacy and safety of multipotent adult progenitor cells (invimestrocel) for acute respiratory distress syndrome (ARDS) caused by pneumonia: a randomized, open-label, standard therapy-controlled, phase 2 multicenter study (ONE-BRIDGE). *Stem Cell Res. Ther.* 14 (1), 217.
- Jiang, N., Tian, X., Wang, Q., et al., 2023. Regulation mechanisms and maintenance strategies of stemness in mesenchymal stem cells. *Stem Cell Rev. Rep.* <https://doi.org/10.1007/s12015-023-10658-3>.
- JRK, S., Rangasami, V.K., Samanta, S., Varghese, O.P., Oommen, O.P., 2021. Discrepancies on the role of oxygen gradient and culture condition on mesenchymal stem cell fate. *Adv. Health Mater.* 10 (6), e2002058.
- Kircher, M., Gambhir, S., Grimm, J., 2011. Noninvasive cell-tracking methods. *Nat. Rev. Clin. Oncol.* 8 (11), 677–688.
- Li, H., Lim, H.C., Zacharaki, D., et al., 2020. Early growth response 1 regulates hematopoietic support and proliferation in human primary bone marrow stromal cells. *Haematologica* 105 (5), 1206–1215.
- Li, M., Jiang, Y., Hou, Q., Zhao, Y., Zhong, L., Fu, X., 2022. Potential pre-activation strategies for improving therapeutic efficacy of mesenchymal stem cells: current status and future prospects. *Stem Cell Res. Ther.* 13 (1), 146.
- Li, X., Hong, Y., He, H., et al., 2019. FGF21 mediates mesenchymal stem cell senescence via regulation of mitochondrial dynamics. *Oxid. Med. Cell. Longev.* 2019, 4915149.
- Liang, Y., Zhou, R., Liu, X., et al., 2022. Leukemia inhibitory factor facilitates self-renewal and differentiation and attenuates oxidative stress of BMSCs by activating PI3K/AKT signaling. *Oxid. Med. Cell. Longev.* 2022, 5772509.
- Liu, J., He, J., Ge, L., et al., 2021. Hypoxic preconditioning rejuvenates mesenchymal stem cells and enhances neuroprotection following intracerebral hemorrhage via the miR-326-mediated autophagy. *Stem Cell Res. Ther.* 12 (1), 413.
- Liu, Z., Wang, H., Wang, Y., et al., 2012. The influence of chitosan hydrogel on stem cell engraftment, survival and homing in the ischemic myocardial microenvironment. *Biomaterials* 33 (11), 3093–3106.
- Ma, Q., Yang, J., Huang, X., et al., 2018. Poly(lactide-co-glycolide)-monomethoxy-poly(polyethylene glycol) nanoparticles loaded with melatonin protect adipose-derived stem cells transplanted in infarcted heart tissue. *Stem Cells* 36 (4), 540–550.
- Maridas, D.E., DeMambro, V.E., Le, P.T., Mohan, S., Rosen, C.J., 2017. IGFBP4 is required for adipogenesis and influences the distribution of adipose depots. *Endocrinology* 158 (10), 3488–3500.
- Mazini, L., Rochette, L., Amine, M., Malka, G., 2019. Regenerative capacity of adipose derived stem cells (ADSCs), comparison with mesenchymal stem cells (MSCs). *Int. J. Mol. Sci.* 20 (10).
- Meyerrose, T., Ugarte, D., Hofling, A., et al., 2007. In vivo distribution of human adipose-derived mesenchymal stem cells in novel xenotransplantation models. *Stem Cells* 25 (1), 220–227.
- Mihai, B.P., Ana-Mihaela, L., Carmen, A.N., et al., 2020. Evidence of mesenchymal stromal cell adaptation to local microenvironment following subcutaneous transplantation. *J. Cell. Mol. Med.* 24 (18), 10889–10897.
- Mohamed, A.G., Ayman, F.R., Batoul, L.E., Mahmoud, M.G., Mahmoud, M.Z., 2020. From mesenchymal stromal/stem cells to insulin-producing cells: progress and challenges. *Stem Cell Rev. Rep.* 16 (6), 1156–1172.
- Moya, A., Paquet, J., Deschepper, M., et al., 2018. Human mesenchymal stem cell failure to adapt to glucose shortage and rapidly use intracellular energy reserves through glycolysis explains poor cell survival after implantation. *Stem Cells* 36 (3), 363–376.
- Niklason, L.E., 2018. Understanding the extracellular matrix to enhance stem cell-based tissue regeneration. *Cell Stem Cell* 22 (3), 302–305.
- Oh, J., Lee, Y.D., Wagers, A.J., 2014. Stem cell aging: mechanisms, regulators and therapeutic opportunities. *Nat. Med.* 20 (8), 870–880.
- Ohta, Y., Takenaga, M., Hamaguchi, A., et al., 2018. Isolation of adipose-derived stem/stromal cells from cryopreserved fat tissue and transplantation into rats with spinal cord injury. *Int. J. Mol. Sci.* 19 (7).
- Pagella, P., de Vargas Roditi, L., Stadlinger, B., Moor, A.E., Mitsiadis, T.A., 2021. Notch signaling in the dynamics of perivascular stem cells and their niches. *Stem Cells Transl. Med.* 10 (10), 1433–1445.
- Qiao, Y., Xu, Z., Yu, Y., et al., 2020. Single cell derived spheres of umbilical cord mesenchymal stem cells enhance cell stemness properties, survival ability and therapeutic potential on liver failure. *Biomaterials* 227, 119573.
- Qiu, S., Sun, Y., Xu, J., et al., 2019. Ferulic acid improves self-renewal and differentiation of human tendon-derived stem cells by upregulating early growth response 1 through hypoxia. *Genesis* 57 (9), e23291.
- Scadden, D.T., 2006. The stem-cell niche as an entity of action. *Nature* 441 (7097), 1075–1079.
- Shi, Y., Inoue, H., Wu, J.C., Yamanaka, S., 2017. Induced pluripotent stem cell technology: a decade of progress. *Nat. Rev. Drug Discov.* 16 (2), 115–130.
- Shuai, Y., Liao, L., Su, X., et al., 2016. Melatonin treatment improves mesenchymal stem cells therapy by preserving stemness during long-term in vitro expansion. *Theranostics* 6 (11), 1899–1917.
- Song, Y., Du, H., Dai, C., et al., 2018. Human adipose-derived mesenchymal stem cells for osteoarthritis: a pilot study with long-term follow-up and repeated injections. *Regen. Med.* 13 (3), 295–307.
- Suh, S., Kim, J., Shin, J., et al., 2004. Use of omentum as an in vivo cell culture system in tissue engineering. *ASAIO J.* 50 (5), 464–467.
- Tamama, K., Barbeau, D.J., 2012. Early growth response genes signaling supports strong paracrine capability of mesenchymal stem cells. *Stem Cells Int.* 2012, 428403.
- Tratwal, J., Mathiasen, A.B., Juhl, M., Brorsen, S.K., Kastrup, J., Ekblond, A., 2015. Influence of vascular endothelial growth factor stimulation and serum deprivation on gene activation patterns of human adipose tissue-derived stromal cells. *Stem Cell Res. Ther.* 6 (1), 62.
- Tsai, C.C., Su, P.F., Huang, Y.F., Yew, T.L., Hung, S.C., 2012. Oct4 and Nanog directly regulate Dnmt1 to maintain self-renewal and undifferentiated state in mesenchymal stem cells. *Mol. Cell* 47 (2), 169–182.
- Valerio, D.N., 2019. Omentum a powerful biological source in regenerative surgery. *Regen. Ther.* 8 (11), 182–191.
- Wang, C., Li, X., Dang, H., Liu, P., Zhang, B., Xu, F., 2019. Insulin-like growth factor 2 regulates the proliferation and differentiation of rat adipose-derived stromal cells via IGF-1R and IR. *Cyotherapy* 21 (6), 619–630.
- Wang, S., Wang, Z., Su, H., et al., 2021. Effects of long-term culture on the biological characteristics and RNA profiles of human bone-marrow-derived mesenchymal stem cells. *Mol. Ther. Nucleic Acids* 26, 557–574.
- Weng, Z., Wang, Y., Ouchi, T., et al., 2022. Mesenchymal stem/stromal cell senescence: hallmarks, mechanisms, and combating strategies. *Stem Cells Transl. Med.* 11 (4), 356–371.
- Yang, J., Sun, L., Han, J., Zheng, W., Peng, W., 2019. DUSP1/MKP-1 regulates proliferation and apoptosis in keratinocytes through the ERK/Elk-1/Egr-1 signaling pathway. *Life Sci.* 223, 47–53.
- Yew, T.L., Chiu, F.Y., Tsai, C.C., et al., 2011. Knockdown of p21(Cip1/Waf1) enhances proliferation, the expression of stemness markers, and osteogenic potential in human mesenchymal stem cells. *Aging Cell* 10 (2), 349–361.
- Youssef, A., Aboalola, D., Han, V.K., 2017. The roles of insulin-like growth factors in mesenchymal stem cell niche. *Stem Cells Int.* 2017, 9453108.
- Yu, C., Kormmuller, A., Brown, C., Hoare, T., Flynn, L.E., 2017. Decellularized adipose tissue microcarriers as a dynamic culture platform for human adipose-derived stem/stromal cell expansion. *Biomaterials* 120, 66–80.
- Zhang, Y., Wang, D., Xu, J., et al., 2019. Stat3 activation is critical for pluripotency maintenance. *J. Cell. Physiol.* 234 (2), 1044–1051.
- Zhao, K., Lin, R., Fan, Z., et al., 2022. Mesenchymal stromal cells plus basiliximab, calcineurin inhibitor as treatment of steroid-resistant acute graft-versus-host disease: a multicenter, randomized, phase 3, open-label trial. *J. Hematol. Oncol.* 15 (1), 22.
- Zhou, N., Li, Q., Lin, X., et al., 2016. BMP2 induces chondrogenic differentiation, osteogenic differentiation and endochondral ossification in stem cells. *Cell Tissue Res.* 366 (1), 101–111.
- Zhou, T., Yuan, Z., Weng, J., et al., 2021. Challenges and advances in clinical applications of mesenchymal stromal cells. *J. Hematol. Oncol.* 14 (1), 24.
- Zhou, W., Lin, J., Zhao, K., et al., 2019. Single-cell profiles and clinically useful properties of human mesenchymal stem cells of adipose and bone marrow origin. *Am. J. Sports Med.* 47 (7), 1722–1733.
- Zhuang, W., Lin, Y., Su, L., et al., 2021. Mesenchymal stem/stromal cell-based therapy: mechanism, systemic safety and biodistribution for precision clinical applications. *J. Biomed. Sci.* 28 (1), 28.